3 Biotech (2025) 15:315
https://doi.org/10.1007/s13205-025-04445-9

ORIGINAL ARTICLE

Protective efficacy of emodin in Swiss Albino mice induced with Dalton Ascitic lymphoma

Jesse Joel[1] · Harish Babu Kolla[2,3] · Sai Rupini Vemuri[4] · Jagadish Kumar Suluvoy[2] · Avany Balasubramanian[1] · Gilbert Ross Rex[5] · Prakash Narayana Reddy[2,3,6] · Srikanth Koigoora[7]

Received: 25 January 2025 / Accepted: 16 June 2025 / Published online: 25 August 2025
© King Abdulaziz City for Science and Technology 2025

Abstract

Emodin is a plant-derived natural compound with potential anti-cancer/tumor properties. In this study, we have evaluated the therapeutic efficacy of emodin as an anti-lymphoma drug in vivo in the Swiss Albino mice induced with Dalton Ascitic lymphoma (DAL). The Swiss Albino mice were induced with lymphoma by injecting the DAL cells intraperitonially and treated with the emodin or a standard drug methotrexate or a vehicle. Emodin has shown a significant therapeutic efficacy in controlling the overall DAL pathology and this was determined through gross pathology, serology, hematology, and histopathological readouts. Emodin reduced the tumor weight, volume, WBC count, and liver damage biomarkers like ALP and AST. It further reduced the inflammation at the portal areas in the liver and its associated inflammation scores. In summary, our findings show that the emodin has shown its therapeutic efficacy in controlling lymphoma in vivo highlighting its efficacy as an anti-lymphoma drug. Furthermore, the in silico analysis has shown that emodin as a potential drug candidate for lymphoma based on the Lipinski's rule of 5 and molecular docking studies.

Keywords Dalton Ascitic lymphoma · Anti-tumor · Drug · Emodin · Pathology · In vivo · In silico

Introduction

Lymphoma is a type of tumor characterized by the continuous and uncontrolled proliferation of lymphoid tissues in the body (Jiang et al. 2017; Zhao et al. 2021). It poses a significant global health burden due to high mortality and morbidity rates (Chu et al. 2023). Clinically, lymphoma is treated with chemo- and radiotherapy (Anand et al. 2024). However, these approaches have their limitations, such as drug resistance, minimal efficacy, severe side effects, or toxicity due to the nature of treatments. These challenges highlight the immediate requirement for novel and effective drugs or therapeutics to enhance the current lymphoma treatment with minimal side effects.

In this context, plant-derived natural compounds have gained attention for treating cancers because of their relatively lower toxicity and diverse biological activities ranging from anti-cancer/anti-tumor to immunomodulatory, antimicrobial, and anti-inflammatory agents. One such molecule is emodin, a natural anthraquinone mostly derived from aloe vera, Rheum sp and Chinese Goldthread, etc. (Dong et al. 2020; Stompor-Goracy 2021) and can induce apoptosis and inhibiting cell proliferation in cancer cells (Zhang et al.

Jesse Joel and Harish Babu Kolla have contributed equally and share first authorship.

✉ Jagadish Kumar Suluvoy
jagadishbabu77@gmail.com

1 Department of Biotechnology, Karunya Institute of Technology and Sciences, Coimbatore, Tamil Nadu, India

2 Department of Biotechnology, Vignan's Foundation for Science, Technology, and Research, Guntur, Andhra Pradesh, India

3 Dr.V.S. Krishna Government Degree College, Maddilapalem, Visakhapatnam, Andhra Pradesh, India

4 Manipal School of Life Sciences, Manipal Academy of Higher Education, Manipal, Udupi, Karnataka, India

5 Department of Biotechnology, Vivekananda College of Engineering for Women, Namakkal, Tamil Nadu, India

6 Microbiology Department, SKR & SKR Govt. College for Women (A), Kadapa, Andhra Pradesh, India

7 Vignan Institute of Technology and Science, Hyderabad, Telangana, India

2020) making it a potent therapeutic option with further study to treat lymphoma.

Furthermore, using murine lymphoma models such as Dalton's Ascitic Lymphoma (DAL)-induced models provides a valuable platform to study the disease pathogenesis, and test and evaluate the anti-lymphoma drugs in laboratory settings (Debnath et al. 2018). DAL is a well-characterized and studied model of T-cell lymphoma that resembles the lymphoid malignancies in patients. This platform offers insight into the progression of tumors and studies the therapeutic effect of various drugs before translating them into patient treatment. Moreover, previous studies have shown that the DAL can be effectively induced in the Swiss Albino mice and lead to the development of human-like lymphoma pathological condition, thus offering a better murine model to study lymphoma pathogenesis and develop effective drugs (Zhou et al. 2023a, b).

In this study, we investigated the in vivo therapeutic efficacy of emodin in DAL-induced Swiss Albino mice through gross pathology, hematology, biochemical assays, histopathology, and in silico approaches. Our findings highlight that emodin treatment has significantly controlled the severity and outcomes of DAL in the mouse model.

Materials and methods

Materials

Cell line, drugs, and chemicals

The DAL cell line was purchased from the National Centre for Cell Sciences, Pune, India. The cells were cultured in the complete Dulbecco's modified Eagle's medium (DMEM) supplemented with 1% penicillin, streptomycin, and 10% fetal calf serum. Methotrexate was purchased from IPCA Laboratories (Mumbai, India). > 90% pure and HPLC-determined synthetic emodin compound was outsourced from Sigma, and all the other chemicals were procured from Merck. The emodin was dissolved in the 0.5% sodium carboxymethyl cellulose for experimental use (Liu et al. 2021a, b).

Animals

The Swiss Albino mice weighing 20–25 g were purchased from Kerala Veterinary and Animal Sciences University, Pookode, Wayanad, Kerala, India. Animals were housed in polyacrylic cages with 6 animals in each cage and bedded with rice hulls. All the animals were acclimatized under the standard laboratory conditions at 25 °C ± 2 °C with proper ventilation and a 12-h daylight cycle throughout the study period. All the animal procedures and protocols were performed between December 2020 and February 2021 based on the standard methods according to the internal animal house guidelines of Vignan's Foundation for Science, Technology, and Research (Reg. No.: 2046/PO/ReBi/S/18/CPCSEA) and Karunya Institute of Technology and Sciences (IAEC/KU/BT/15/08) as per Committee for the Purpose of Control and Supervision of Experiments on Animals guidelines, Government of India.

Cell culture

The DAL cells were thawed in a water bath upon receipt from the supplier. The cells were washed with sterile, chilled 1X PBS to remove dimethylsulfoxide and other stabilizers from the cells. The quality of the cells was determined through the trypan blue method before seeding them in a flask for culturing. The DAL cells were seeded in a T-25 flask with 5 mL of completed DMEM and passed to a fresh flask at 85% confluency.

Anti-lymphoma study

A total of 36 mice were used in this study. The animals were divided into 6 groups at 6 animals per group as follows: Group I—DAL + PBS; Group II—normal + PBS; Group III— DAL + 50 mg/kg of emodin; Group IV—DAL + 100 mg/kg of emodin; Group V—DAL + 150 mg/kg of emodin; Group VI—DAL + Methotrexate (Kumar And Berlin Grace 2016). Six animals were left uninduced with DAL, while the others were induced with DAL by injecting around 1.5×10^6 cells/mice through the intraperitoneal route (Fig. 1). The emodin dose and the type of vehicle were chosen based on the prior studies on its in vivo studies (Feng et al. 2010; Xiong et al. 2019; Akkol et al. 2021; Liu et al. 2021a, b; Zheng et al. 2021; Zhu et al. 2021). The animals were carefully monitored by the animal care veterinary technician for any uneasiness, illness, or behavior daily. After 15 days of treatment, all the experimental mice were sacrificed once they were confirmed doing well in terms of their health and behavior, and the therapeutic efficacy of emodin was assessed by measuring the tumor, total body measurements, blood parameters, serum profile, and histopathology.

Tumor and total body measurements

All the mice were sacrificed, and the total body weight, tumor weight, and volume were measured after 15 days of treatment with emodin or methotrexate. The tumor weight and volume were measured by collecting the ascitic fluid.

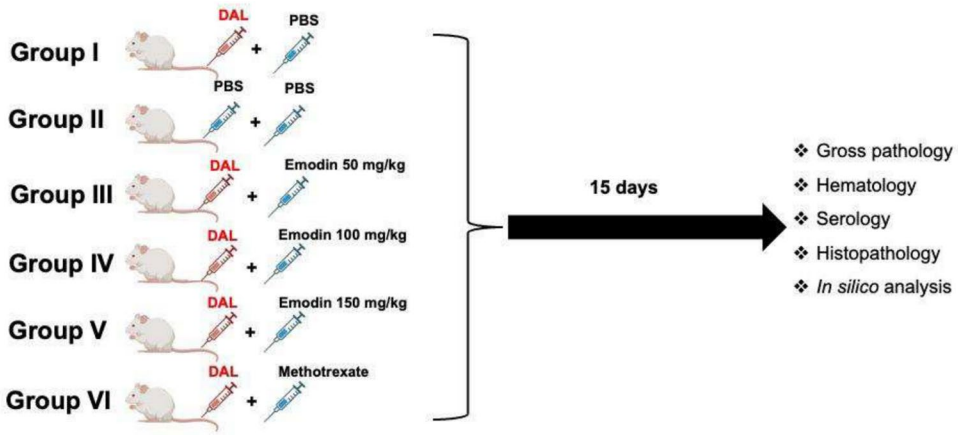


Fig. 1 Schematic representation of the study. Swiss Albino mice were categorized into six groups ($n=6$). Group I—DAL + PBS; Group II—normal + PBS; Group III—DAL + 50 mg/kg of emodin; Group IV—DAL + 100 mg/kg of emodin; Group V—DAL + 150 mg/kg of emodin; Group VI—DAL + Methotrexate. The treatment was continued for 15 days, and they were sacrificed to evaluate the therapeutic efficacy by studying the gross pathology (body weight, morphological examination, tumor weight, and volume), hematology (RBC, hemoglobin, and WBC count), serology (ALP and AST levels), histopathology (liver inflammation), and in silico analysis (drug-likeliness properties and molecular docking studies)

Hematological parameters

Blood was collected from all the mice through cardiac puncture in heparin-coated Eppendorf tubes. The total red blood cells (RBC), hemoglobin content, and white blood cells (WBC) were determined in each sample with the help of a local pathology laboratory as per our previous study (Kumar And Berlin Grace 2016).

Serology

An aliquot of the collected blood was centrifuged at 2000 rpm for 20 min at 4 °C. The serum was isolated and stored at – 80 °C for the biochemical analysis to measure Alkaline Phosphatase (ALP) and aspartate aminotransferase (AST) levels in each mouse using kits procured from Sigma-Aldrich.

Histopathology

The liver tissues from control, normal, and treated groups were fixed in formalin solution for 48 h, washed twice with ethanol, and sent to a local pathologist for paraffin embedding and sectioning. The sections were stained with hematoxylin and eosin, mounted, and dried overnight. The slides were observed under a light microscope at 40X magnification. The inflammation grade scoring is performed accordingly: 0: no inflammation; 1: mild inflammation with a few scattered inflammatory cells in the portal areas; 2: moderate inflammation with noticeable clusters of inflammatory cells in the portal areas; 3: severe inflammation with dense and widespread infiltrates; 4: very severe inflammation with massive infiltration as per Knodell et al 1981.

In silico analysis

The drug-likeliness properties of emodin were assessed based on the standard Lipinski's rule of 5 using the Swiss ADME tool (http://www.swissadme.ch/). The structural information of emodin and methotrexate was submitted to the server in SMILES format. Further, the molecular docking studies were carried out to investigate the ability of emodin and the standard drug methotrexate to interact and affinity with the key lymphoma drug targets, such as B-cell lymphoma extra-large (Bcl-xL) (PDB ID: 2YXJ), cellular FLICE (FADD-like IL-1β-converting enzyme)-inhibitory protein (c-FLIP) (PDB ID: 3H13), glutathione S transferase (GST) (PDB ID: 2A2R), glutathione reductase (PDB ID: 3DK8), AKT1 (PDB ID: 3O96), map kinase ERK2 (PDB ID: 6G54), matrix metalloproteinase 9 (MMP9) (PDB ID: 4WZV), and signal transducer and activator of transcription 3 (STAT3) (PDB ID: 6NUQ). Molecular docking studies were carried out using the Seam Dock server through Vina module (https://seamless.rpbs.univ-paris-diderot.fr/cloudless/instance/9148275/ctx/index.html) (Murail et al. 2021).

Statistical analysis

The data presented in this manuscript are represented as mean ± SD. Data normality was assessed using the Shapiro–Wilk test before statistical analysis. All statistical analyses were performed using one-way ANOVA in GraphPad

Prism version 10.3.1. Where applicable, multiple comparisons were corrected using Dunnett's test. *P* values were considered statistically significant as follows: $*P<0.05$, $**P<0.01$, $***P<0.001$, $****P<0.0001$.

Results

Gross pathology

Increase in the total body weight because of continuous proliferation of lymphocytes is considered an important readout of lymphoma distending the abdomen in tumor induced mice. The emodin (50 mg/kg: $p<0.0001$; 100 mg/kg: $p<0.0001$; 150 mg/kg: $p<0.0001$) or methotrexate ($p<0.0001$) treatment has shown a significant decrease on the total body weight bringing a notable morphological change in DAL bearing mice and has blunted the enlargement of abdomen in mice (Fig. 2A and B). Similarly, there is almost 40% decrease in the tumor volume (50 mg/kg: $p=0.0001$; 100 mg/kg: $p<0.0001$; 150 mg/kg: $p=0.0005$; methotrexate: $p<0.0001$) and weights (Fig. 2C) in methotrexate ($p=0.0002$) and emodin treatment (50 mg/kg: $p<0.0001$; 100 mg/kg: $p<0.0001$; 150 mg/kg: $p=0.0004$) groups at all the three concentrations. However, the mice received a 100 mg/kg emodin dose have shown a prominent effect in controlling the tumor weight and volume as compared to 50 mg/kg and 150 mg/kg, respectively (Fig. 2C).

Hematology

The total RBC population, hemoglobin content, and WBC population were estimated after sacrifice of all the animals. The RBC count is reduced in the tumor group as compared to the normal group ($p=0.0046$). While the treatment with methotrexate or emodin at 150 mg/kg ($p=0.0046$) has shown a positive effect on the RBC population by significantly increasing the cell count, but not in the other groups (Fig. 3A). Specifically, the total RBC count in the untreated controls is around $2X10^6$/uL. There is no significant change observed in the RBC population with either 50 or 100 mg/kg of emodin treatment. However, their population is increased ~ twofold and is close to the normal levels with 150 mg/kg of emodin treatment (Fig. 3A). A similar trend

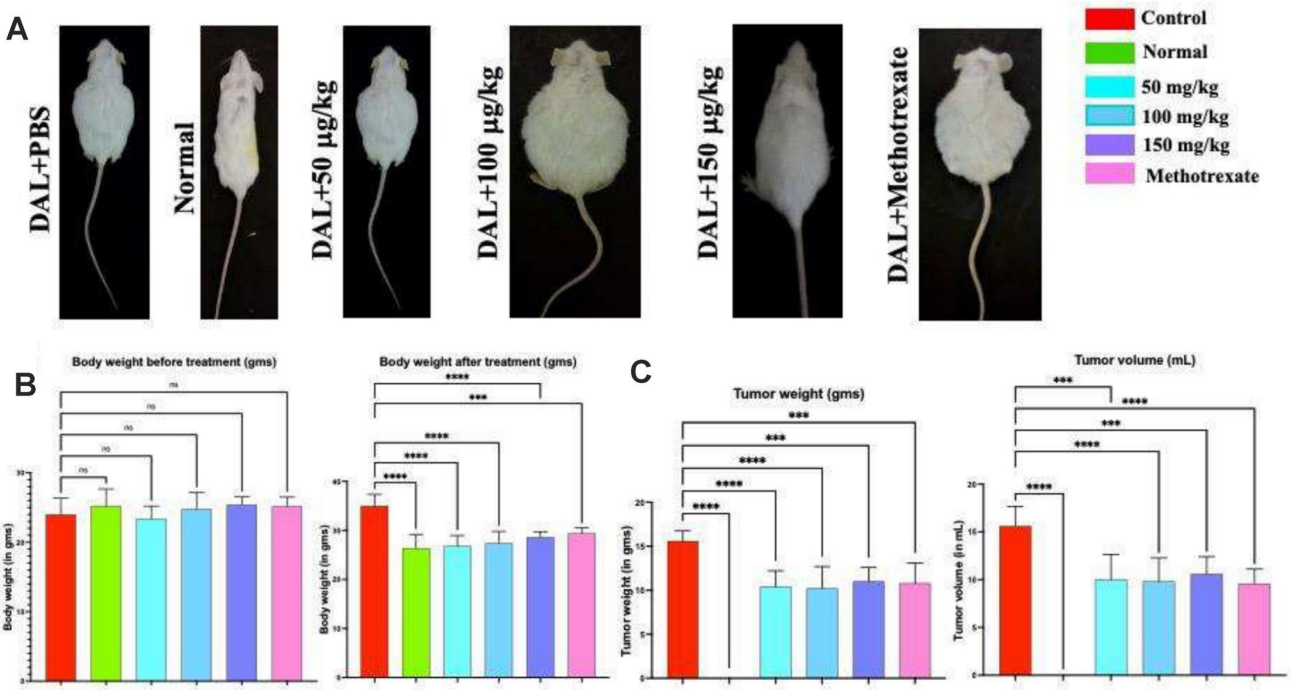


Fig. 2 Therapeutic effect of emodin and methotrexate on the gross pathology of DAL-induced mice. Emodin treatment has improved the gross pathology in DAL-bearing mice. A. Emodin and methotrexate treatment has reduced the swelling in DAL-induced mice; **B** emodin and methotrexate treatment reduced the body weights (50 mg/kg of emodin [$n=6$; $P<0.0001$]; 100 mg/kg of emodin [$n=6$; $P<0.0001$]; 150 mg/kg of emodin [$n=6$; $P<0.0001$]; and methotrexate [$n=6$; $P=0.0003$]); **C** tumor volume (50 mg/kg of emodin [$n=6$; $P=0.0001$]; 100 mg/kg of emodin [$n=6$; $P<0.0001$]; 150 mg/kg of emodin [$n=6$; $P=0.0005$]; and methotrexate [$n=6$; $P<0.0001$]) and weights (50 mg/kg of emodin [$n=6$; $P<0.0001$]; 100 mg/kg of emodin [$n=6$; $P<0.0001$]; 150 mg/kg of emodin [$n=6$; $P=0.0004$]; and methotrexate [$n=6$; $P=0.0002$]) in treated groups. All the data are represented in mean ± SD. *P* values were considered statistically significant as follows: $*P<0.05$, $**P<0.01$, $***P<0.001$, $****P<0.0001$

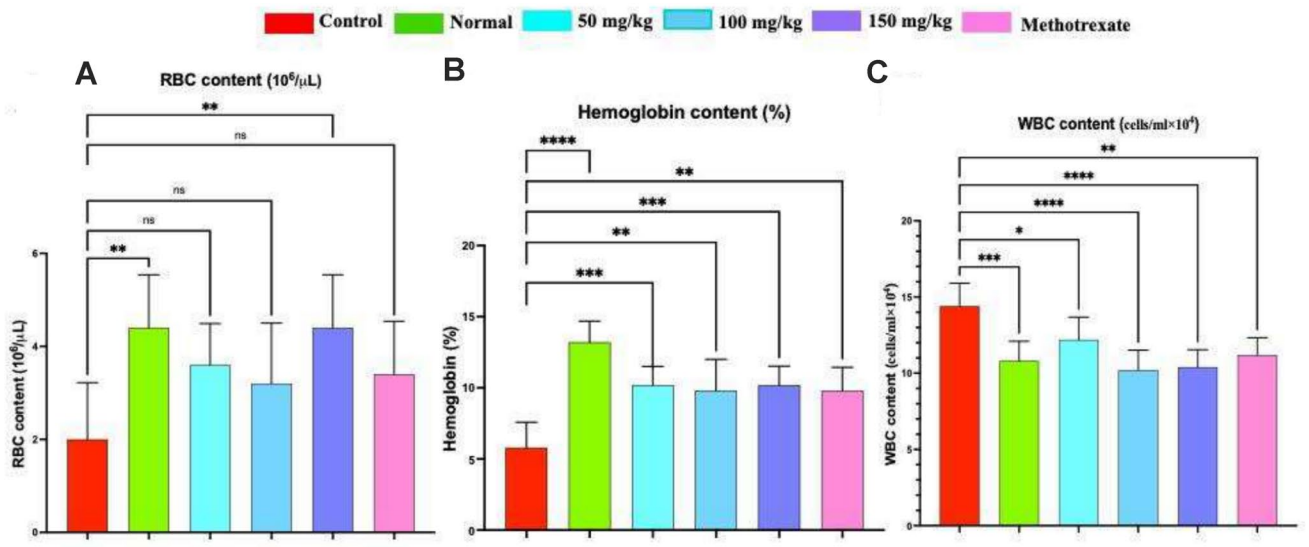


Fig. 3 Therapeutic effect of emodin and methotrexate on the hematological parameters of DAL-induced mice. **A** RBC count (10^6/uL) in 50 mg/kg of emodin [$n=6$; $P=0.0838$]; 100 mg/kg of emodin [$n=6$; $P=0.2668$]; 150 mg/kg of emodin [$n=6$; $P=0.0046$]; and methotrexate [$n=6$; $P=0.1542$]), **B** hemoglobin content (%) in 50 mg/kg of emodin [$n=6$; $P=0.0003$]; 100 mg/kg of emodin [$n=6$; $P=0.0010$]; 150 mg/kg of emodin [$n=6$; $P=0.0003$]; and methotrexate [$n=6$; $P=0.0010$]), **C** WBC count (cells/mLX10.^{4}) in 50 mg/kg of emodin [$n=6$; $P=0.0295$]; 100 mg/kg of emodin [$n=6$; $P<0.0001$]; 150 mg/kg of emodin [$n=6$; $P<0.0001$]; and methotrexate [$n=6$; $P=0.0010$]). All the data represented in mean ± SD. P values were considered statistically significant as follows: $^*P<0.05$, $^{**}P<0.01$, $^{***}P<0.001$, $^{****}P<0.0001$

is seen with emodin treatment on the hemoglobin content among all the groups (Fig. 3B). The percentage of hemoglobin content is significantly increased in all the treatment groups (50 mg/kg: $p=0.0003$; 100 mg/kg: $p=0.0010$; 150 mg/kg: $p=0.0003$; methotrexate: $p=0.0010$) as compared to the control ones. The hemoglobin content is around 5% in the untreated controls. The emodin treatment at all the three doses (50–150 mg/kg) has increased the concentration almost twofold which is close to that in the normal group without lymphoma (Fig. 3B). On the other hand, the emodin treatment has shown its therapeutic effect by reducing the total WBC population at all the concentrations (50 mg/kg: $p=0.0295$; 100 mg/kg: $p<0.0001$; 150 mg/kg: $p<0.0001$) like the methotrexate treatment ($p=0.0010$) (Fig. 3C). In the controls, the WBC population is around 15 cells/mlX10^4, which was leveled to that of the normal group, i.e., 10 cells/mlX10^4, with almost 40% reduction in the total WBC count, indicating the efficacy of emodin in controlling the lymphoma (Fig. 3C). However, the mice treated with either 100 or 150 mg/kg of emodin have shown a better effect in controlling the WBC population as compared to 50 mg/kg (Fig. 3C).

Serology

The serum biomarkers of the liver, such as ALP and AST, are used to monitor the effectiveness of anti-lymphoma chemotherapeutic drugs. We studied how the emodin treatment affected these markers. The levels of ALP ($p<0.0001$) and AST ($p<0.0001$) markers were markedly increased in the tumor groups than those of normal mice (Fig. 4A, B). The levels of these two markers were also greatly reduced in all the treatment groups (ALP [50 mg/kg: $p<0.0001$; 100 mg/kg: $p<0.0001$; 150 mg/kg: $p<0.0001$; methotrexate: $p<0.0001$]; AST [50 mg/kg: $p<0.0001$; 100 mg/kg: $p<0.0001$; 150 mg/kg: $p<0.0001$; methotrexate: $p<0.0001$]) and reached the normal level (Fig. 4A, B).

Histopathology

The liver pathology was studied from the representative animal from each group. The H&E staining revealed that the normal mice have a preserved hepatic lobular architecture and morphology. In contrast, the DAL bearing group with PBS only treatment shows that the portal areas are surrounded by severe fibrosis and massive inflammation (Fig. 5A, B). This pathological condition is relatively reconstituted with a significant reduction in the inflammation scores (50 mg/kg: $p=0.0001$; 100 mg/kg: $p<0.0001$; 150 mg/kg: $p=0.0001$; methotrexate: $p<0.0001$) normal hepatocellular architecture in all the treatment groups (50–150 mg/kg of emodin and methotrexate) evidencing the anti-tumor activity of emodin (Fig. 5C–F). However, there is a slight infiltration observed in the 150 mg/kg emodin-treated group.

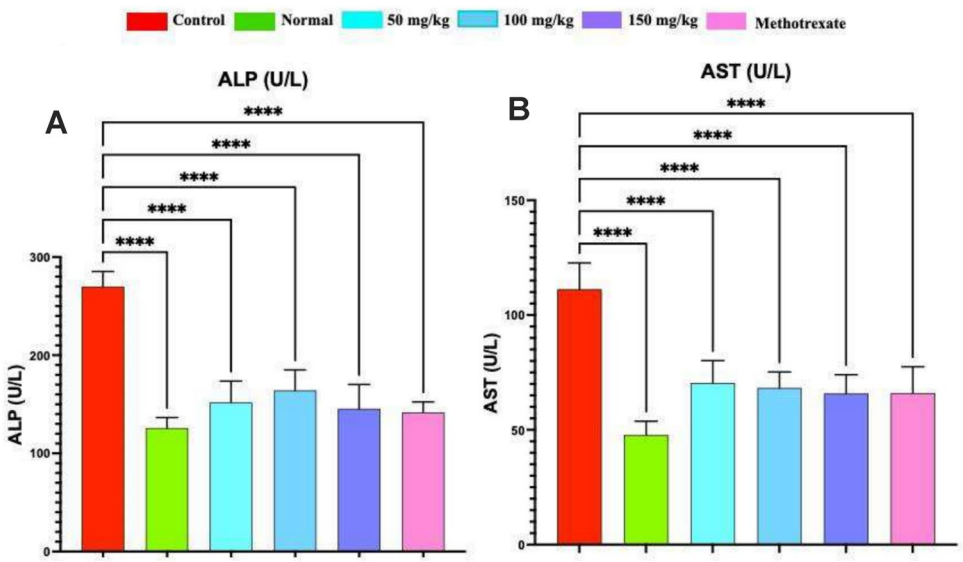


Fig. 4 Therapeutic effect of emodin and methotrexate on the serum biomarkers in DAL-induced mice. A. ALP levels in 50 mg/kg of emodin [$n=6$; $P<0.0001$]; 100 mg/kg of emodin [$n=6$; $P<0.0001$]; 150 mg/kg of emodin [$n=6$; $P<0.0001$]; and methotrexate [$n=6$; $P<0.0001$]), **B** AST levels in 50 mg/kg of emodin [$n=6$; $P<0.0001$]; 100 mg/kg of emodin [$n=6$; $P<0.0001$]; 150 mg/kg of emodin [$n=6$; $P<0.0001$]; and methotrexate [$n=6$; $P<0.0001$]). All the data represented in mean ± SD. P values were considered statistically significant as follows: *$P<0.05$, **$P<0.01$, ***$P<0.001$, ****$P<0.0001$

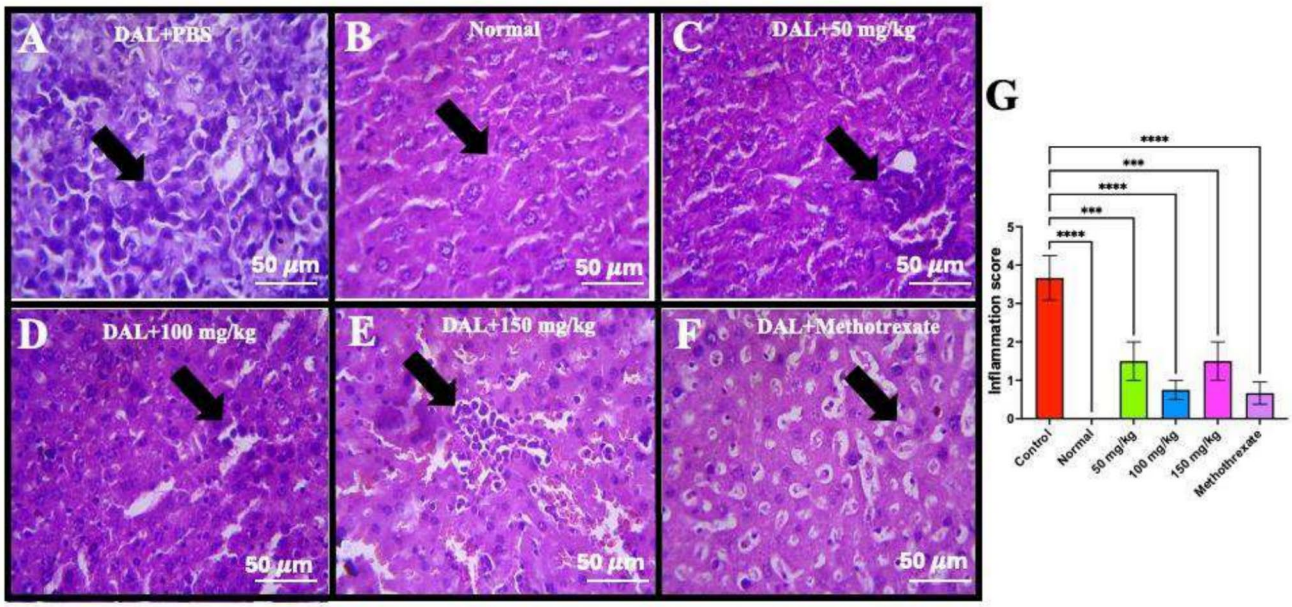


Fig. 5 Histopathological examination of liver sections from the representative mouse in **A** DAL + PBS (control), **B** PBS + PBS (normal), **C** 50 mg/kg of emodin, **D** 100 mg/kg of emodin, **E.** 150 mg/kg of emodin, **F** and methotrexate-treated groups. **G** Emodin (50 mg/kg: $n=6$, $p<0.0001$; 100 mg/kg: $n=6$, $p<0.0001$; 150 mg/kg: $n=6$, $p<0.0001$) and methotrexate treatments ($n=6$; $p<0.0001$) have significantly reduced the inflammation scores in the liver sections. All the data represented in mean ± SD. P values were considered statistically significant as follows: *$P<0.05$, **$P<0.01$, ***$P<0.001$, ****$P<0.0001$

Drug likeliness

The drug-likeliness properties of the emodin compound were assessed based on Lipinski's rule of five-molecular weight, hydrogen bond donors, acceptors, and LogP values. Apparently, emodin has matched all the criteria of Lipinski's rules with less than 5 H-donors, molecular weight of less than 500 g/mol, and less than 10 H-bond acceptors, and with a LogP value of less than 5 (Fig. 6). All these values were compared with the standard drug methotrexate, and the emodin was found to be a better drug candidate to treat lymphoma.

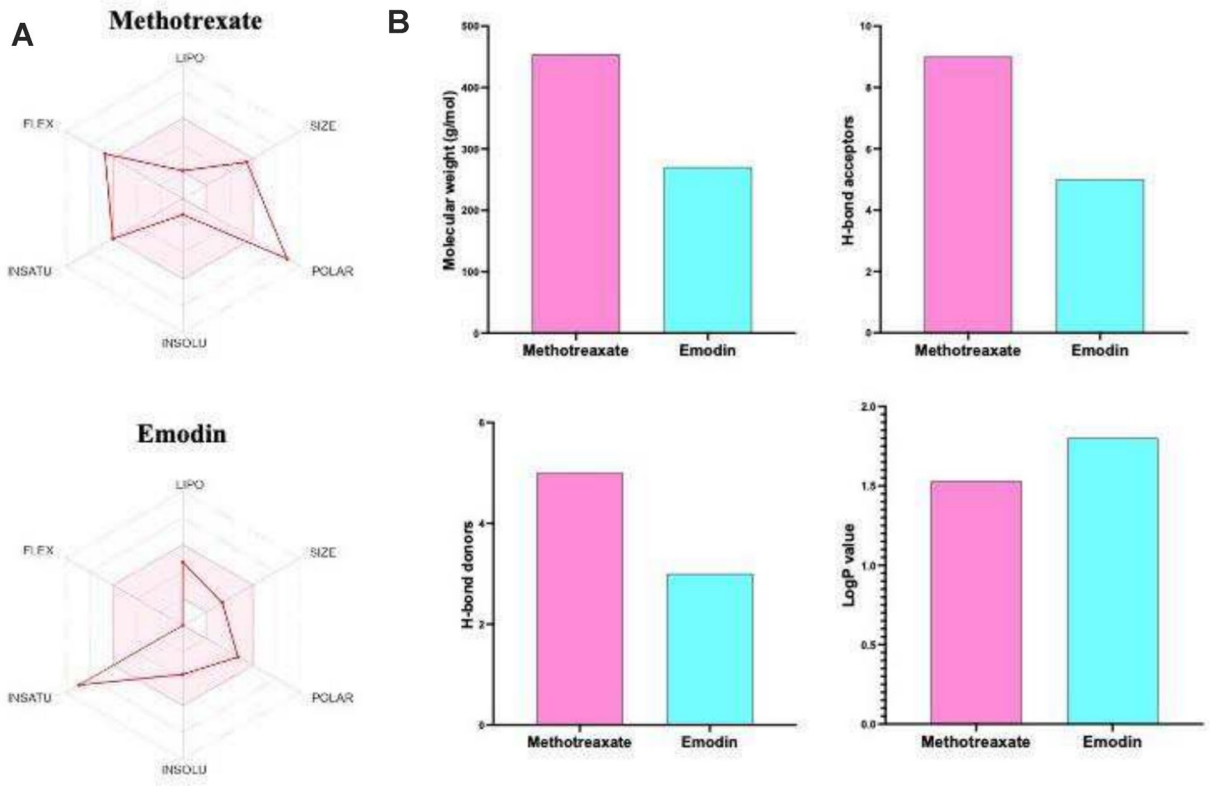


Fig. 6 Drug likeliness profile of emodin and methotrexate compounds. **A** Swiss MADE map of emodin, **B** Swiss ADME map of methotrexate, and **C** Lipinski's rule of five parameters of emodin and methotrexate

Molecular docking analysis

The inhibitory action of potential anti-lymphoma drugs is always correlated with their affinity to the target receptor (Devidas et al. 2021; Kumar et al. 2023; Singh et al. 2024). We have chosen Bcl-xL, c-FLIP, GST, AKT1, MMP9, glutathione reductase, ERK2, and STAT3 as potential targets for molecular docking studies based on their central roles in lymphoma pathogenesis. The Bcl-XL and c-FLIP are anti-apoptotic proteins that are overexpressed in lymphoma and thereby contribute to resistance toward apoptosis (Mathas et al. 2004; Oyarzo et al. 2006; Morales-Martinez And Vega 2022; Liu et al. 2023). On the other hand, GST and glutathione reductase are involved in the detoxification and maintaining redox balance in the cell (Alnasser 2025; de Cubas et al. 2025). Overactivity of these enzymes supports drug resistance and tolerance toward oxidative stress in lymphoma, which emodin may disrupt through pro-oxidant activity (Bennaceur-Griscelli et al. 2004; Luersen et al. 2013; Bernig et al. 2016). Similarly, AKT1 and ERK2 are key kinases in the PI3K/AKT and MAPK/ERK pathways, which are upregulated in lymphoma to promote tumor proliferation and survival (Zheng et al. 2003; Rudelius et al. 2006; Zhang et al. 2022). MMP9 facilitates the invasion of tumors by degrading the extracellular matrix (Cottam And Rees 1993; Stetler-Stevenson 2001; Fang et al. 2003; Khasigov et al. 2003; Halbersztadt et al. 2006; Augoff et al. 2022). STAT3 is persistently activated in lymphoma (Zhu et al. 2019), drives oncogenic gene expression linked to survival, angiogenesis, and immune evasion, and is another known target of emodin.

The emodin has shown a promising interaction with these targets with a strong Gibbs free energy (ΔG) values of – 10.4 (AKT); – 7.9 (Bcl-XL); – 7.1 (c-FLIP); – 8.6 (ERK2); – 8.3 (Glutathione reductase); – 8.1 (Glutathione transferase); – 8.5 (MMP9); – 8.2 (STAT3), respectively (Fig. 7), stabilized by the hydrophobic interactions (AKT-4; Bcl-XL-5; c-FLIP-3; ERK2-5; Glutathione reductase-1; Glutathione transferase-1; MMP9-7; and STAT3-3) and H-bonds (AKT-4; Bcl-XL-5; c-FLIP-6; ERK2-4; Glutathione reductase-11; Glutathione transferase-5; MMP9-8; and STAT3-9) as shown in the Fig. 7 and Table 1.

The docking analysis was further carried out between the standard drug methotrexate and the same targets. The methotrexate bound to these targets efficiently with affinities of – 10 (AKT); – 8.0 (Bcl-XL); – 7.0 (c-FLIP); – 8.8 (ERK2); – 9.7 (Glutathione reductase); – 8.1 (Glutathione transferase); – 10.0 (MMP9); – 8.3 (STAT3) respectively (Fig. 8) stabilized by the hydrophobic interactions (AKT-4; Bcl-XL-4; c-FLIP-1; ERK2-4; Glutathione reductase-1;

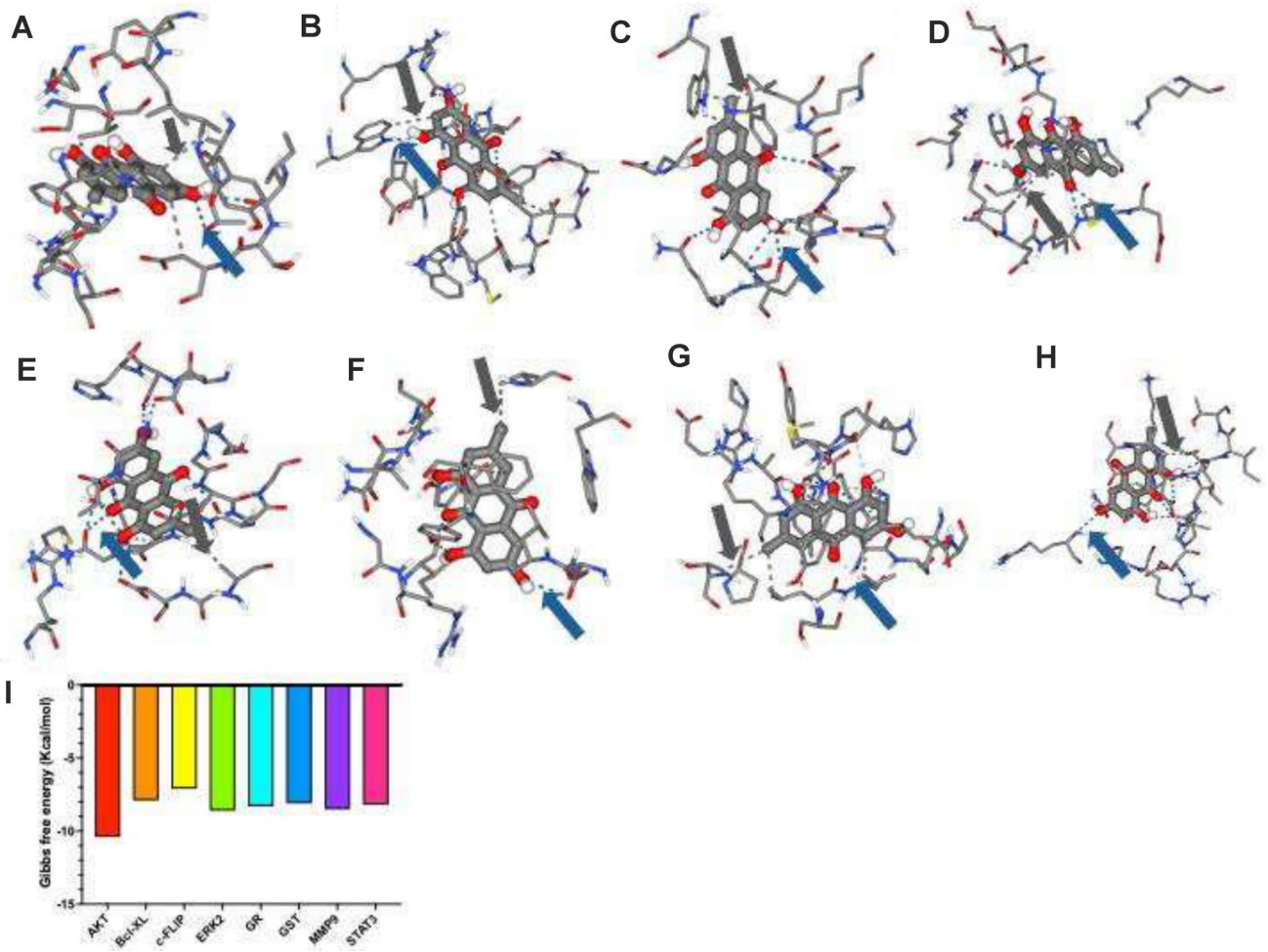


Fig. 7 Molecular docking studies of emodin with **A** AKT, **B** Bcl-XL, **C** c-FLIP, **D** glutathione reductase, **E** glutathione transferase, **F** map kinase ERK2. **G** matrix metalloproteinase. **H** Signal transducer and activator of transcription 3 STAT3 with their respective binding affinities (**I**). The blue arrows indicate H-bonds and gray arrows showing hydrophobic interactions between the ligand and receptor

Glutathione transferase-1; MMP9-3; and STAT3-2) and H-bonds (AKT-9; Bcl-XL-1; c-FLIP-1; ERK2-7; Glutathione reductase-1; Glutathione transferase-8; MMP9-8; and STAT3-13) as shown in the Fig. 8 and Table 2.

Discussion

In the present study, we studied the anti-lymphoma activity of emodin in the Swiss albino mice model induced with the DAL ascites. DAL offers several advantages over the other models of lymphoma, like EL4 and A20, for the preclinical screening of anti-lymphoma drugs. DAL is rapidly progressing with high tumor or ascitic fluid yield and strong response to the chemotherapies (Sriram et al. 2010). While EL4 and A20, which are typically used in immunocompetent C57BL/6 and BALB/c mice and require longer experimental durations, DAL allows for quicker assessment of drug efficacy due to its aggressive nature, making it an ideal model for evaluating cytotoxic potential in a time- and cost-efficient manner (https://www.labcorp.com/education-events/articles/a20-modeling-b-cell-lymphoma-mice). Additionally, the ease of propagation and reproducibility of the DAL model make it well suited for high-throughput in vivo studies. While not optimal for immunotherapy research due to its limited immunogenicity, DAL remains a valuable tool for early phase screening of anti-cancer compounds targeting lymphoma.

Our findings highlight the therapeutic potential of emodin in controlling the severity of lymphoma in DAL-induced murine model by reducing the tumor burden, which is studied through several readouts. Emodin is a natural anthraquinone molecule derived from various plant sources (Stompor-Goracy 2021). It has been studied for its anti-cancer activity primarily because of its ability to induce apoptosis in the cancer cells and eliminate them (Zhang et al. 2020).

Table 1 Two-dimensional interactions between the emodin and docking targets

Hydrophobic		Hydrogen bond		Gibbs free energy (Kcal/mol)
Ligand	Receptor	Ligand	Receptor	
AKT				
C9	W80(A) CB	O5	T211(A) O	– 10.4
C14	L210(A) CB	O5	T211(A) OG1	
C12	V270(A) CG1	O5	I290(A) O	
C11	D292(A) CB	O5	T211(A) OG1	
Bcl-XL				
C12	F123(A) CE2	O3	E124(A) OE2	– 7.9
C7	E124(A) CG	O1	W169(A) O	
C15	V127(A) CB	O4	D176(A) OD2	
C12	Y173(A) CD2	O5	P116(B) O	
C14	W169(B) CZ2	O4	W169(B) NE1	
c-FLIP				
C15	L422(A) CD2	O5	L412(A) O	– 7.1
C15	W453(A) CZ3	O4	Q415(A) OE1	
C9	W453(A) CH2	O5	S416(A) O	
		O5	S419(A) O	
		O3	P420(A) O	
		O3	Y463(A) OH	
ERK2				
C12	I31(A) CB	O1	I31(A) O	– 8.6
C1	I31(A) CD	O5	Q105(A) OE1	
C3	V39(A) CG1	O3	M108(A) O	
C11	A52(A) CB	O3	M108(A) N	
C11	L156(A) CD1			
Glutathione reductase				
C15	A342(A) CB	O5	E50(A) OE2	– 8.3
		O2	T57(A) OG1	
		O1	T57(A) OG1	
		O3	A155(A) O	
		O4	G158(A) O	
		O2	G158(A) O	
		O1	D331(A) OD1	
		O2	T57(A) OG1	
		O1	T57(A) OG1	
		O1	G158(A) N	
		O5	S51(A) OG	
GST				
C15	V35(A) CG2	O2	Y7(A) OH	– 8.1
		O4	Y7(A) OH	
		O5	Q51(A) OE1	
		O1	Y108(A) OH	
		O4	Y7(A) OH	
MMP9				
C7	L222(A) CB	O2	H226(A) ND1	– 8.5
C15	L222(A) CD2	O1	A242(A) O	
C11	V223(A) CG2	O1	L243(A) O	
C4	H226(A) CB	O1	Y245(A) O	
C9	L243(A) CD1	O2	M247(A) O	
C4	Y248(A) CD1	O1	M247(A) O	
C15	T251(A) CG2	O2	H226(A) ND1	
		O4	H226(A) NE2	
STAT3				
C15	K370(A) CB	O2	D369(A) OD1	– 8.2
C12	L438(A) CB	O1	D369(A) OD1	
C4	V490(A) CG2	O5	R379(A) N	
		O2	L436(A) O	
		O4	L436(A) O	
		O1	L438(A) N	
		O1	L438(A) O	
		O5	N491(A) OD1	
		O1	L438(A) N	

Our results indicate that the emodin exhibited its anti-tumor nature by reducing body weight, tumor weight, and volumes in the DAL bearing mice upon treatment. As an immunosuppressive agent (Qiu et al. 2020), the main aspect of emodin's action against lymphoma lies in its ability to reduce the WBC/lymphocyte population, which is observed with the reduction or control of the WBC population by emodin in our later results in the hematology experiments.

Another important property of emodin's action is its anti-inflammatory properties, which are evident from our serology and liver histopathological observations (Han et al. 2015; Li et al. 2020; Cheng et al. 2022; Saha And Ahmad 2024). The liver tissue is characterized by the presence of massive infiltration of immune cells and tissue necrosis with an increase in the liver damage biomarkers such as ALP and AST, which could promote the growth of tumors and metastasis. We found that the emodin treatment reduced the immune cell infiltration with a remarkable reduction in ALP and AST, highlighting its anti-inflammatory nature, which might be attributed to the down-regulation of the nuclear factor kappa B pathway, which is chronically activated in malignancies and contributes to severe inflammation and tissue damage (Zhu et al. 2023). Furthermore, the in silico analysis has also shown that the likelihood of emodin as a potential anti-lymphoma drug.

The molecular docking studies corroborate various experimental validations for its interactions with the selected targets. Emodin was identified to downregulate the expression of Bcl-xl and further promote the mitochondrial-mediated apoptosis in various cancer models (Su et al. 2005; Zu et al. 2015; Li et al. 2019; Saunders et al. 2019), which is

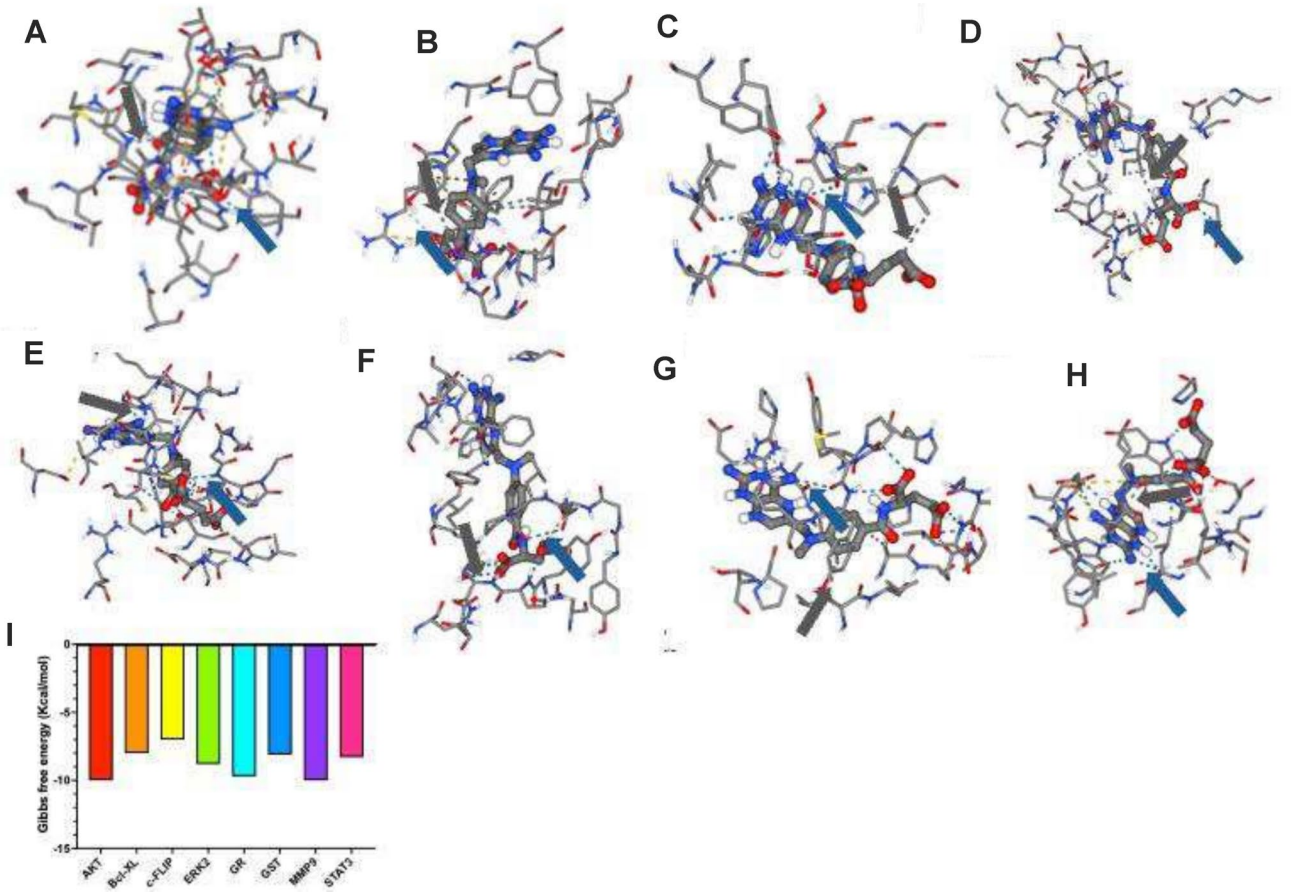


Fig. 8 Molecular docking studies of methotrexate with **A** AKT, **B** Bcl-XL, **C.** c-FLIP, **D** glutathione reductase, **E** glutathione transferase, and **F** map kinase ERK2. **G** Matrix metalloproteinase. **H** Signal transducer and activator of transcription 3 STAT3 with their respective binding affinities (**I**). The blue arrows indicate H-bonds and gray arrows showing hydrophobic interactions between the ligand and receptor

consistent with the strong docking score in our study. Binding of inhibitor/ligand at the functional domains of Bcl-XL would likely interrupt its ability to sequester the pro-apoptotic proteins like BAX/BAK (Kang And Reynolds 2009; Rong et al. 2009; Westphal et al. 2014; Lopez et al. 2022). This facilitates the formation of the apoptosome and caspase activation to polarize the apoptosis in cancer cells. Similarly, c-FLIP is another suppressor of extrinsic apoptosis by inhibiting caspase-8 at the death-inducing signaling complex (Chang et al. 2002). Emodin suppresses the expression of c-FLIP and sensitizes the cancer cells to apoptosis (Subramaniam et al. 2013). The predicted ligand interactions from this study might block its recruitment and inhibit its function. Apart from this, emodin has been reported to deplete glutathione and disrupt cellular redox balance in cancer cells (Wang et al. 2010; Li et al. 2016). Inhibition of GST and GR disrupts the redox homeostasis in cancer cells and elevates oxidative stress in cancer cells, making them susceptible to ROS-mediated apoptosis (Arfin et al. 2021). This supports our findings of the interaction of emodin with these enzymes. Emodin is known to attenuate the PI3K/AKT pathway by inhibiting AKT1 phosphorylation (Olsen et al. 2007) and suppressing the expression of its downstream targets like mTOR (Zheng et al. 2019), GSK-3β (Hu et al. 2016), ERK2 (Chang et al. 2016), and STAT3 (Wang et al. 2019). We presume that the emodin binds to AKT1, blocks the ATP binding, or stabilizes its inactive state. This can collectively weaken growth signals with increased susceptibility to apoptosis. Moreover, the inhibition of EKR2 attenuates the signal transduction from RTKs and suppresses the expression of cyclins and anti-apoptotic genes (Roy et al. 2010; Tunoglu et al. 2024; Wei et al. 2025). In various cancer models, the MMP9 activity is known to be inhibited by emodin (Kim et al. 2005; Chen et al. 2010; Liu et al. 2021a, b). Our docking analysis indicates the direct interaction of emodin to its catalytic zinc-binding domain, which could impair its proteolytic activity and reduce metastasis. And finally, any ligand interference with the STAT3 dimerization or DNA-binding domains restricts its nuclear translocation and transcriptional activity of anti-apoptotic and proliferative genes like Bcl-2,

Table 2 Two-dimensional interactions between the methotrexate and docking targets

Hydrophobic interactions		Hydrogen bond		Gibbs free energy (Kcal/mol)
Ligand	Receptor	Ligand	Receptor	
AKT				
C12	Q79(A) CB	N4	T82(A) OG1	– 10.0
C11	W80(A) CB	O5	S205(A) OG	
C2	W80(A) CE3	N7	Y272(A) OH	
C6	V270(A) CG1	N6	D274(A) OD1	
		N3	D292(A) OD2	
		N4	T82(A) OG1	
		O2	N53(A) ND2	
		O5	S205(A) OG	
		O3	W80(A) N	
Bcl-XL				
C4	F97(B) CD2	O3	G138(B) O	– 8.0
C4	Y101(B) CE2			
C8	L130(B) CD1			
C8	A142(B)			
c-FLIP				
C4	T264(A) CG2	N8	Y360(A) OH	– 7.0
			L412(A) O	
			Q415(A) OE1	
			S416(A) O	
			S418(A) O	
			S418(A) OG	
			S418(A) OG	
			S419(A) O	
			S419(A) O	
			S419(A) OG	
			P420(A) O	
			Y463(A) OH	
			Y463(A) OH	
			Y463(A) OH	
			Y463(A) OH	
			S418(A) OG	
			S419(A) OG	
			S418(A) OG	
ERK2				
C11	I31(A) CB	O4	S41(A) OG	– 8.8
C2	I31(A) CG2	N6	Q105(A) OE1	
C12	I31(A) CD	O3	M108(A) O	
C2	L107(A) CD2	O1	E109(A) O	
		O1	E109(A) OE2	
		N5	D167(A) OD1	
		O4	S41(A) OG	
Glutathione reductase				
C4	A342(A) CB	O1	S30(A) OG	– 9.7
		O3	S30(A) OG	
		N7	G56(A) O	
		O2	T57(A) OG1	
		O5	A155(A) O	
		O4	V329(A) O	
		O1	T339(A) OG1	
		O2	T57(A) OG1	
		O4	G157(A) N	
		O5	G31(A) N	
		O1	S30(A) OG	
		O1	T339(A) OG1	
		O3	S30(A) N	
		O3	C58(A) N	
		O3	S30(A) OG	
GST				
C4	Q51(A) CB	N2	Q51(A) OE1	– 8.1
		O1	S65(A) OG	
		O3	S65(A) OG	
		N6	G205(A) O	
		O5	Q64(A) N	
		O1	S65(A) OG	
		O3	S65(A) N	
		O3	S65(A) OG	
MMP9				
C8	L222(A) CB	O4	A189(A) O	– 10.0
C6	H226(A) CB	O4	E227(A) OE1	
C11	Y248(A) CD1	N6	P240(A) O	
		N4	E241(A) O	
		O1	P246(A) O	
		N7	M247(A) O	
		O5	L188(A) N	
		O3	Y248(A) N	
STAT3				
C8	A505(A) CB	N3	D502(A) OD2	– 8.3
C6	L525(A) CD1	O1	E506(A) O	
		O2	S509(A) OG	
		O3	S509(A) OG	
		N8	T526(A) OG1	
		N5	T526(A) OG1	
		N8	V537(A) O	
		N7	S540(A) OG	
		N5	T526(A) OG1	
		O2	S509(A) OG	
		O5	W510(A) NE1	
		O3	S509(A) OG	
		O3	S513(A) OG	

and survivin (Yang et al. 2022). Findings from these studies support the molecular docking predictions and suggest a multi-target mechanism through which emodin exerts anti-lymphoma effects. These correlations validate the computational findings and highlight the therapeutic potential of emodin as a multi-faceted anti-cancer agent.

While our study highlights the anti-lymphoma activity of emodin, there are several limitations as well. First, the DAL model resembles the human lymphoma pathology in clinical settings but does not completely replicate it. Future studies in vitro on its cytotoxicity, anti-proliferative apoptosis assays, and in-depth mechanistic studies in the patient tumor-derived cell line study might answer this question. Since emodin can modulate multiple pathways in the cancer pathogenesis, more studies on its ability to modulate those pathways in controlling the lymphoma would be highly appreciated. Furthermore, in-depth investigation of the pharmacokinetics, pharmacodynamics, and metabolism of emodin in the body will be critical in standardizing the optimal dosage for clinical application. However, recent studies show that the emodin has a moderate bioavailability (Zhou et al. 2023a, b) and limited absorption (Zheng et al. 2021) and a significant first-pass metabolism through glucuronidation and sulfation in the liver (Shen et al. 2022; Song et al. 2022). From the in vivo studies, it was identified that the emodin reaches maximum plasma concentration within 9 min post-administration (Peng et al. 2008). Also, its half-life is around 11 h, and its metabolites are primarily excreted via bile and urine (Zhou et al. 2023a, b). These pharmacokinetic characteristics suggest that sustained or repeated dosing may be required to maintain therapeutic levels in vivo. Therefore, incorporating this pharmacological context helps in interpreting efficacy outcomes and guides future in vivo dosing strategies aimed at improving therapeutic impact and bioavailability.

Conclusion

In this study, we investigated the anti-lymphoma activity of emodin in the DAL-induced Swiss Albino mouse model. The mice-bearing lymphoma has shown an improved therapeutic outcome with emodin treatment at different doses of 50 mg/kg, 100 mg/kg, and 150 mg/kg. Emodin treatment significantly reduced the tumor burden in the mice with reduction in the tumor weight, volume, and abdominal swelling. The mice have shown a decrease in the total WBC count and the liver damage markers like ALP and AST. Similarly, the histopathological analysis has shown that the emodin treatment has reduced the overall leukocyte infiltration near the portal areas and inflammation in the liver tissue. These findings were compared along with a standard drug methotrexate treatment. The drug-likeliness properties of emodin were compared along with the methotrexate and docking studies. The in silico analysis has shown emodin possess all the five rules of Lipinski's and has shown a strong interaction with the potential anti-lymphoma targets. Overall, emodin has shown a better or considerable therapeutic activity in our study by controlling the severity of lymphoma in comparison with the methotrexate. However, further in-depth mechanistic and clinical studies are required to evaluate its safety before translating this molecule for lymphoma therapy.

Author contributions JJ planned and performed the experiments. HBK performed experiments, analyzed the data, wrote, and revised the manuscript. SRV performed data analysis and revised the manuscript. JKS performed experiments and wrote the manuscript. AB performed experiments and wrote the manuscript. GRR, PNR, and SK performed the docking analysis and significant revisions in the manuscript.

Funding Not applicable.

Data availability statement All the data generated in this study in included in the manuscript. The raw data is provided upon request made to the corresponding author.

Declarations

Conflict of interest The authors declare that there is no conflict of interest.

Ethical approval All the experiments carried out in the current study were according to the guidelines from Institutional Animal Ethics Committee, of Vignan's Foundation for Science, Technology, and Research (Reg. No.: 2046/PO/ReBi/S/18/CPCSEA), Guntur, Andhra Pradesh, India.

Consent to participate Not applicable.

Consent for publication Authors declare that there is no conflict of interest.

References

Akkol EK, Tatli II, Karatoprak GS, Agar OT, Yucel C, Sobarzo-Sanchez E, Capasso R (2021) Is emodin with anticancer effects completely innocent? Two Sides of the Coin. Cancers (Basel) 13:2733. https://doi.org/10.3390/cancers13112733

Alnasser SM (2025) The role of glutathione S-transferases in human disease pathogenesis and their current inhibitors. Genes Dis 12:101482. https://doi.org/10.1016/j.gendis.2024.101482

Anand U, Dey A, Singh Chandel AK, Sanyal R, Mishra A, Pandey DK, De Falco V, Upadhyay A, Kandimalla R, Chaudhary A, Dhanjal JK, Dewanjee S, Vallamkondu J, Perez de la Lastra JM (2024) Corrigendum to: cancer chemotherapy and beyond: current status, drug candidates, associated risks and progress in targeted therapeutics. Genes Dis 11:101211. https://doi.org/10.1016/j.gendis.2024.101211

Arfin S, Jha NK, Jha SK, Kesari KK, Ruokolainen J, Roychoudhury S, Rathi B, Kumar D (2021) Oxidative stress in cancer cell metabolism. Antioxid (Basel) 10:642. https://doi.org/10.3390/antiox10050642

Augoff K, Hryniewicz-Jankowska A, Tabola R, Stach K (2022) MMP9: a tough target for targeted therapy for cancer. Cancers (Basel) 14:1847. https://doi.org/10.3390/cancers14071847

Bennaceur-Griscelli A, Bosq J, Koscielny S, Lefrere F, Turhan A, Brousse N, Hermine O, Ribrag V (2004) High level of glutathione-S-transferase pi expression in mantle cell lymphomas. Clin Cancer Res 10:3029–3034. https://doi.org/10.1158/1078-0432.CCR-03-0554

Bernig T, Ritz S, Brodt G, Volkmer I, Staege MS (2016) Glutathione-S-transferases and chemotherapy resistance of Hodgkin's lymphoma cell lines. Anticancer Res 36:3905–3915

Chang DW, Xing Z, Pan Y, Algeciras-Schimnich A, Barnhart BC, Yaish-Ohad S, Peter ME, Yang X (2002) c-FLIP(L) is a dual function regulator for caspase-8 activation and CD95-mediated apoptosis. EMBO J 21:3704–3714. https://doi.org/10.1093/emboj/cdf356

Chang X, Zhao J, Tian F, Jiang Y, Lu J, Ma J, Zhang X, Jin G, Huang Y, Dong Z, Liu K, Dong Z (2016) Aloe-emodin suppresses esophageal cancer cell TE1 proliferation by inhibiting AKT and ERK phosphorylation. Oncol Lett 12:2232–2238. https://doi.org/10.3892/ol.2016.4910

Chen YY, Chiang SY, Lin JG, Ma YS, Liao CL, Weng SW, Lai TY, Chung JG (2010) Emodin, aloe-emodin and rhein inhibit migration and invasion in human tongue cancer SCC-4 cells through the inhibition of gene expression of matrix metalloproteinase-9. Int J Oncol 36:1113–1120. https://doi.org/10.3892/ijo_00000593

Cheng L, Chen J, Rong X (2022) Mechanism of emodin in the treatment of rheumatoid arthritis. Evid Based Complement Alternat Med 2022:9482570. https://doi.org/10.1155/2022/9482570

Chu Y, Liu Y, Fang X, Jiang Y, Ding M, Ge X, Yuan D, Lu K, Li P, Li Y, Xu H, Fan J, Zhou X, Wang X (2023) The epidemiological patterns of non-Hodgkin lymphoma: global estimates of disease burden, risk factors, and temporal trends. Front Oncol 13:1059914. https://doi.org/10.3389/fonc.2023.1059914

Cottam D, Rees R (1993) Regulation of matrix metalloproteinases – their role in tumor invasion and metastasis. Int J Oncol 2:861–872

de Cubas L, Boronat S, Vega M, Domenech A, Gomez-Armengol F, Artemov A, Lyublinskaya O, Ayte J, Hidalgo E (2025) The glutathione system maintains the thiol redox balance in the mitochondria of fission yeast. Free Radic Biol Med 234:100–112. https://doi.org/10.1016/j.freeradbiomed.2024.12.017

Debnath S, Mukherjee A, Karan S, Debnath M, Chatterjee TK (2018) Induction of apoptosis, anti-proliferation, tumor-angiogenic suppression and down-regulation of Dalton's Ascitic Lymphoma (DAL) induced tumorigenesis by poly-L-lysine: a mechanistic study. Biomed Pharmacother 102:1064–1076. https://doi.org/10.1016/j.biopha.2018.03.079

Devidas SB, Rahmatkar SN, Singh R, Sendri N, Purohit R, Singh D, Bhandari P (2021) Amelioration of cognitive deficit in zebrafish by an undescribed anthraquinone from *Juglans regia* L.: an in-silico, in-vitro and in-vivo approach. Eur J Pharmacol 906:174234

Dong X, Zeng Y, Liu Y, You L, Yin X, Fu J, Ni J (2020) Aloe-emodin: a review of its pharmacology, toxicity, and pharmacokinetics. Phytother Res 34:270–281. https://doi.org/10.1002/ptr.6529

Fang W, Li H, Kong L, Niu G, Gao Q, Zhou K, Zheng J, Wu B (2003) Role of matrix metalloproteinases (MMPs) in tumor invasion and metastasis: serial studies on MMPs and TIMPs. Beijing Da Xue Xue Bao Yi Xue Ban 35:441–443 ((**in Chinese**))

Feng Y, Huang SL, Dou W, Zhang S, Chen JH, Shen Y, Shen JH, Leng Y (2010) Emodin, a natural product, selectively inhibits 11β-hydroxysteroid dehydrogenase type 1 and ameliorates metabolic disorder in diet-induced obese mice. Br J Pharmacol 161:113–126. https://doi.org/10.1111/j.1476-5381.2010.00866.x

Halbersztadt A, Halon A, Pajak J, Robaczynski J, Rabczynski J, St Gabrys M (2006) The role of matrix metalloproteinases in tumor invasion and metastasis. Ginekol Pol 77:63–71 ((**in Polish**))

Han JW, Shim DW, Shin WY, Heo KH, Kwak SB, Sim EJ, Jeong JH, Kang TB, Lee KH (2015) Anti-inflammatory effect of emodin via attenuation of NLRP3 inflammasome activation. Int J Mol Sci 16:8102–8109. https://doi.org/10.3390/ijms16048102

https://www.labcorp.com/education-events/articles/a20-modeling-b-cell-lymphoma-mice

Hu C, Dong T, Li R, Lu J, Wei X, Liu P (2016) Emodin inhibits epithelial to mesenchymal transition in epithelial ovarian cancer cells by regulation of GSK-3β/β-catenin/ZEB1 signaling pathway. Oncol Rep 35:2027–2034. https://doi.org/10.3892/or.2015.4527

Jiang M, Bennani NN, Feldman AL (2017) Lymphoma classification update: T-cell lymphomas, Hodgkin lymphomas, and histiocytic/dendritic cell neoplasms. Expert Rev Hematol 10:239–249. https://doi.org/10.1080/17474086.2017.1286090

Kang MH, Reynolds CP (2009) Bcl-2 inhibitors: targeting mitochondrial apoptotic pathways in cancer therapy. Clin Cancer Res 15:1126–1132. https://doi.org/10.1158/1078-0432.CCR-08-0144

Khasigov PZ, Podobed OV, Gracheva TS, Salbiev KD, Grachev SV, Berezov TT (2003) Role of matrix metalloproteinases and their inhibitors in tumor invasion and metastasis. Biochemistry (Mosc) 68:711–717. https://doi.org/10.1023/A:1025068412085

Kim MS, Park MJ, Kim SJ, Lee CH, Yoo H, Shin SH, Song ES, Lee SH (2005) Emodin suppresses hyaluronic acid-induced MMP-9 secretion and invasion of glioma cells. Int J Oncol 27:839–846. https://doi.org/10.3892/ijo.27.3.839

Knodell RG, Ishak KG, Black WC et al (1981) Formulation and application of a numerical scoring system for assessing histological activity in asymptomatic chronic active hepatitis. Hepatology 1(5):431–435

Kumar SJ, Berlin Grace VM (2016) Anti-lymphoma activity of *Averrhoa bilimbi* fruit extract in Swiss albino mice. Asian J Pharm 10(2):S183

Kumar S, Bhardwaj VK, Singh R, Purohit R (2023) Structure restoration and aggregate inhibition of V30M mutant transthyretin protein by potential quinoline molecules. Int J Biol Macromol 231:123318

Li X, Wang H, Wang J, Chen Y, Yin X, Shi G, Li H, Hu Z, Liang X (2016) Emodin enhances cisplatin-induced cytotoxicity in human bladder cancer cells through ROS elevation and MRP1 downregulation. BMC Cancer 16:578. https://doi.org/10.1186/s12885-016-2591-7

Li C, Gao S, Yang WS, Jin GZ, Sun S (2019) β-Dihydroartemisinin-emodin promotes apoptosis by activating extrinsic and intrinsic pathways in human liver cancer cells. Ann Clin Lab Sci 49:281–290

Li Q, Gao J, Pang X, Chen A, Wang Y (2020) Molecular mechanisms of action of emodin: as an anti-cardiovascular disease drug. Front Pharmacol 11:559607. https://doi.org/10.3389/fphar.2020.559607

Liu C, Chen L, Wang W, Qin D, Jia C, Yuan M, Wang H, Guo Y, Zhu J, Zhou Y, Zhao H, Liu T (2021a) Emodin suppresses the migration and invasion of melanoma cells. Biol Pharm Bull 44:771–779. https://doi.org/10.1248/bpb.b20-00953

Liu H, Wang Q, Shi G, Yang W, Zhang Y, Chen W, Wan S, Xiong F, Wang Z (2021b) Emodin ameliorates renal damage and podocyte injury in a rat model of diabetic nephropathy via regulating AMPK/mTOR-mediated autophagy signaling pathway. Diabetes Metab Syndr Obes 14:1253–1266. https://doi.org/10.2147/DMSO.S299660

Liu C, Ding X, Li G, Zhang Y, Shao Y, Liu L, Zhang W, Ma Y, Guan W, Wang L, Xu Z, Chang Y, Zhang Y, Jiang B, Yin Q, Tao R (2023) Targeting Bcl-xL is a potential therapeutic strategy for extranodal NK/T cell lymphoma. iScience 26:107369. https://doi.org/10.1016/j.isci.2023.107369

Lopez A, Reyna DE, Gitego N, Kopp F, Zhou H, Miranda-Roman MA, Nordstrom LU, Narayanagari SR, Chi P, Vilar E, Tsirigos A, Gavathiotis E (2022) Co-targeting of BAX and

BCL-XL proteins broadly overcomes resistance to apoptosis in cancer. Nat Commun 13:1199. https://doi.org/10.1038/s41467-022-28908-8

Luersen K, Stegehake D, Daniel J, Drescher M, Ajonina I, Ajonina C, Hertel P, Woltersdorf C, Liebau E (2013) The glutathione reductase GSR-1 determines stress tolerance and longevity in *Caenorhabditis elegans*. PLoS ONE 8:e60731. https://doi.org/10.1371/journal.pone.0060731

Mathas S, Lietz A, Anagnostopoulos I, Hummel F, Wiesner B, Janz M, Jundt F, Hirsch B, Johrens-Leder K, Vornlocher HP, Bommert K, Stein H, Dorken B (2004) c-FLIP mediates resistance of Hodgkin/Reed-Sternberg cells to death receptor-induced apoptosis. J Exp Med 199:1041–1052. https://doi.org/10.1084/jem.20032079

Morales-Martinez M, Vega MI (2022) Roles and regulation of BCL-xL in hematological malignancies. Int J Mol Sci 23:2083. https://doi.org/10.3390/ijms23042083

Murail S, de Vries SJ, Rey J, Moroy G, Tuffery P (2021) SeamDock: an interactive and collaborative online docking resource to assist small compound molecular docking. Front Mol Biosci 8:716466

Olsen BB, Bjorling-Poulsen M, Guerra B (2007) Emodin negatively affects the phosphoinositide 3-kinase/AKT signalling pathway: a study on its mechanism of action. Int J Biochem Cell Biol 39:227–237. https://doi.org/10.1016/j.biocel.2006.10.008

Oyarzo MP, Medeiros LJ, Atwell C, Feretzaki M, Leventaki V, Drakos E, Amin HM, Rassidakis GZ (2006) c-FLIP confers resistance to FAS-mediated apoptosis in anaplastic large-cell lymphoma. Blood 107:2544–2547. https://doi.org/10.1182/blood-2005-06-2456

Peng J, Shen ZS, Ma C (2008) Emodin studies on pharmacokinetics and distribution in rat liver after *Polygonum cuspidatum* Sieb. et Zucc. extract administration. World Sci Technol 10:64–67

Qiu F, Liu H, Liang CL, Nie GD, Dai Z (2020) Corrigendum: A new immunosuppressive molecule emodin induces both CD4(+)FoxP3(+) and CD8(+)CD122(+) regulatory T cells and suppresses murine allograft rejection. Front Immunol 11:1381. https://doi.org/10.3389/fimmu.2020.01381

Rong YP, Barr P, Yee VC, Distelhorst CW (2009) Targeting Bcl-2 based on the interaction of its BH4 domain with the inositol 1,4,5-trisphosphate receptor. Biochim Biophys Acta 1793:971–978. https://doi.org/10.1016/j.bbamcr.2009.02.005

Roy SK, Srivastava RK, Shankar S (2010) Inhibition of PI3K/AKT and MAPK/ERK pathways causes activation of FOXO transcription factor, leading to cell cycle arrest and apoptosis in pancreatic cancer. J Mol Signal 5:10. https://doi.org/10.1186/1750-2187-5-10

Rudelius M, Pittaluga S, Nishizuka S, Pham TH, Fend F, Jaffe ES, Quintanilla-Martinez L, Raffeld M (2006) Constitutive activation of Akt contributes to the pathogenesis and survival of mantle cell lymphoma. Blood 108(5):1668–1676. https://doi.org/10.1182/blood-2006-02-004945

Saha P, Ahmad F (2024) Neuroprotective, anti-inflammatory and anti-fibrillogenic offerings by emodin against Alzheimer's dementia: a systematic review. ACS Omega 9(7):7296–7309. https://doi.org/10.1021/acsomega.3c08579

Saunders IT, Mir H, Kapur N, Singh S (2019) Emodin inhibits colon cancer by altering BCL-2 family proteins and cell survival pathways. Cancer Cell Int 19:98. https://doi.org/10.1186/s12935-019-0813-8

Shen P, Han L, Chen G, Cheng Z, Liu Q (2022) Emodin attenuates acetaminophen-induced hepatotoxicity via the cGAS-STING pathway. Inflammation 45(1):74–87. https://doi.org/10.1007/s10753-021-01541-3

Singh R, Manna S, Nandanwar H, Purohit R (2024) Bioactives from medicinal herb against bedaquiline resistant tuberculosis: removing the dark clouds from the horizon. Microbes Infect 26(3):105279

Song Y, Yang J, Wang X, Chen J, Si D, Gao H, Sun M, Cheng X, Wei F, Ma S (2022) Pharmacokinetics and metabolism of trans-emodin dianthrones in rats. J Ethnopharmacol 290:115123. https://doi.org/10.1016/j.jep.2022.115123

Sriram MI, Kanth SB, Kalishwaralal K, Gurunathan S (2010) Antitumor activity of silver nanoparticles in Dalton's lymphoma ascites tumor model. Int J Nanomed 5:753–762. https://doi.org/10.2147/IJN.S11249

Stetler-Stevenson WG (2001) The role of matrix metalloproteinases in tumor invasion, metastasis, and angiogenesis. Surg Oncol Clin N Am 10(2):383–392. https://doi.org/10.1016/S1055-3207(18)30153-2

Stompor-Gorący M (2021) The health benefits of emodin, a natural anthraquinone derived from rhubarb—a summary update. Int J Mol Sci 22(17):9522. https://doi.org/10.3390/ijms22179522

Su YT, Chang HL, Shyue SK, Hsu SL (2005) Emodin induces apoptosis in human lung adenocarcinoma cells through a reactive oxygen species-dependent mitochondrial signaling pathway. Biochem Pharmacol 70(2):229–241. https://doi.org/10.1016/j.bcp.2005.04.010

Subramaniam A, Loo SY, Rajendran P, Manu KA, Perumal E, Li F, Shanmugam MK, Siveen KS, Park JI, Ahn KS, Hui KM, Kumar AP, Sethi G (2013) An anthraquinone derivative, emodin sensitizes hepatocellular carcinoma cells to TRAIL-induced apoptosis through the induction of death receptors and downregulation of cell survival proteins. Apoptosis 18(10):1175–1187. https://doi.org/10.1007/s10495-013-0863-7

Tunoglu S, Tutar L, Gumus M, Tunoglu ENY, Koca I, Tutar Y (2024) Hsp inhibitor is affective against adenocarcinomic human alveolar basal epithelial cells through modulating ERK/MAPK signaling pathway. Chem Biodivers 21(2):e202301422. https://doi.org/10.1002/cbdv.202301422

Wang W, Sun YP, Huang XZ, He M, Chen YY, Shi GY, Li H, Yi J, Wang J (2010) Emodin enhances sensitivity of gallbladder cancer cells to platinum drugs via glutathione depletion and MRP1 downregulation. Biochem Pharmacol 79(8):1134–1140. https://doi.org/10.1016/j.bcp.2009.11.022

Wang Z, Chen H, Chen J, Hong Z, Liao Y, Zhang Q, Tong H (2019) Emodin sensitizes human pancreatic cancer cells to EGFR inhibitor through suppressing Stat3 signaling pathway. Cancer Manag Res 11:8463–8473. https://doi.org/10.2147/CMAR.S210440

Wei R, Pan X, Cai D, Pan L (2025) Synergistic inhibition of breast carcinoma cell proliferation by quercetin and sulforaphane via activation of the ERK/MAPK pathway. Cell Biochem Biophys. https://doi.org/10.1007/s12013-024-01263-4

Westphal D, Kluck RM, Dewson G (2014) Building blocks of the apoptotic pore: how Bax and Bak are activated and oligomerize during apoptosis. Cell Death Differ 21(2):196–205. https://doi.org/10.1038/cdd.2013.75

Xiong G, Chen H, Wan Q, Dai J, Sun Y, Wang J, Li X (2019) Emodin promotes fibroblast apoptosis and prevents epidural fibrosis through PERK pathway in rats. J Orthop Surg Res 14(1):319. https://doi.org/10.1186/s13018-019-1344-z

Yang J, Wang L, Guan X, Qin JJ (2022) Inhibiting STAT3 signaling pathway by natural products for cancer prevention and therapy: In vitro and in vivo activity and mechanisms of action. Pharmacol Res 182:106357. https://doi.org/10.1016/j.phrs.2022.106357

Zhang N, Wang J, Sheng A, Huang S, Tang Y, Ma S, Hong G (2020) Emodin inhibits the proliferation of MCF-7 human breast cancer cells through activation of aryl hydrocarbon receptor (AhR). Front Pharmacol 11:622046. https://doi.org/10.3389/fphar.2020.622046

Zhang X, Wu Y, Sun X, Cui Q, Bai X, Dong G, Gao Z, Wang Y, Gao C, Sun S, Ji N, Liu Y (2022) The PI3K/AKT/mTOR signaling pathway is aberrantly activated in primary central nervous system lymphoma and correlated with a poor prognosis. BMC Cancer 22(1):190. https://doi.org/10.1186/s12885-022-09174-7

Zhao H, Wu L, Yan G, Chen Y, Zhou M, Wu Y, Li Y (2021) Inflammation and tumor progression: signaling pathways and targeted

intervention. Signal Transduct Target Ther 6(1):263. https://doi.org/10.1038/s41392-021-00622-3

Zheng B, Fiumara P, Li YV, Georgakis G, Snell V, Younes M, Vauthey JN, Carbone A, Younes A (2003) MEK/ERK pathway is aberrantly active in Hodgkin disease: a signaling pathway shared by CD30, CD40, and RANK that regulates cell proliferation and survival. Blood 102(3):1019–1027. https://doi.org/10.1182/blood-2002-11-3557

Zheng XY, Yang SM, Zhang R, Wang SM, Li GB, Zhou SW (2019) Emodin-induced autophagy against cell apoptosis through the PI3K/AKT/mTOR pathway in human hepatocytes. Drug des Devel Ther 13:3171–3180. https://doi.org/10.2147/DDDT.S205042

Zheng Q, Li S, Li X, Liu R (2021) Advances in the study of emodin: an update on pharmacological properties and mechanistic basis. Chin Med 16(1):102. https://doi.org/10.1186/s13020-021-00329-4

Zhou L, Hu X, Han C, Niu X, Han L, Yu H, Pan G, Fu Z (2023a) Comprehensive investigation on the metabolism of emodin both in vivo and in vitro. J Pharm Biomed Anal 223:115122. https://doi.org/10.1016/j.jpba.2022.115122

Zhou Y, Xia J, Xu S, She T, Zhang Y, Sun Y, Wen M, Jiang T, Xiong Y, Lei J (2023b) Experimental mouse models for translational human cancer research. Front Immunol 14:1095388. https://doi.org/10.3389/fimmu.2023.1095388

Zhu F, Wang KB, Rui L (2019) STAT3 activation and oncogenesis in lymphoma. Cancers (Basel). https://doi.org/10.3390/cancers12010022

Zhu YP, Song YR, Quan W, Xu XX, Cui YY, Hu XH, Li XZ (2021) Letter to the editor: administration of TGF-ss inhibitor mitigates radiation-induced fibrosis in a mouse model. Clin Orthop Relat Res 479(8):1862–1863. https://doi.org/10.1097/CORR.0000000000001462

Zhu X, Guo S, Zhang M, Bai X (2023) Emodin protects against apoptosis and inflammation by regulating reactive oxygen species-mediated NF-kappaB signaling in interleukin-1beta-stimulated human nucleus pulposus cells. Hum Exp Toxicol 42:9603271221138552. https://doi.org/10.1177/09603271221138552

Zu C, Zhang M, Xue H, Cai X, Zhao L, He A, Qin G, Yang C, Zheng X (2015) Emodin induces apoptosis of human breast cancer cells by modulating the expression of apoptosis-related genes. Oncol Lett 10(5):2919–2924. https://doi.org/10.3892/ol.2015.3615

Springer Nature or its licensor (e.g. a society or other partner) holds exclusive rights to this article under a publishing agreement with the author(s) or other rightsholder(s); author self-archiving of the accepted manuscript version of this article is solely governed by the terms of such publishing agreement and applicable law.